

## NUMERICAL ANALYSIS OF THE INFLUENCE OF STIR ON WATER DURING MICROWAVE HEATING

Y. Jian, X. Q. Yang, and K. M. Huang

College of Electronics and Information Engineering  
Sichuan University, Chengdu, Sichuan 610065, China

**Abstract**—In order to study the information of temperature with stir during microwave heating on water, the coupled Maxwell's equations, fluid field equations and heat transport equations were solved using Finite-Element Method (FEM). The microwave heating on water was analyzed with high power, different dynamic viscosities and relative complex permittivities. The results show that the highest temperature occurs on the interface of the water and air. When the water is heated under high microwave power, speeding up the stir can improve the uniform of temperature, but if the rotate speed is fast enough, going on speeding up the stir cannot decrease the temperature difference any more. When the value of the imaginary part of relative complex permittivity which accounts for dielectric losses or the dynamic viscosity increases, the temperature in the water rises very quickly, and the temperature difference is very large even if the rotate speed is fast enough.

### 1. INTRODUCTION

Currently, more and more interesting methods are used for heating materials such as microwave heating and induction heating [1]. Unlike other heat sources such as conventional heating, where heat is applied externally to the surface of the material, microwave irradiation penetrates and simultaneously heats the bulk of the material. Referring to Metaxas, Meredith, Saltiel and Datta for an introduction to heat and mass transfers in microwave processing, a number of other analyses of the microwave heating process have appeared in the recent literature [2–9]. Currently, microwaves are widely used in chemical industry to accelerate chemical reactions [10]. However,

since the interaction between chemical reactions and microwave has not been fully understood, the mechanisms of many special effects such as hotspots and thermal run-away are not yet crystal clear, and the possible existence of non-thermal effect is under discussion. The dangers caused by hotspots in the microwave heating cannot be ignored. For example, it was found in our previous researches that specific phenomena such as explosion which took place during the crystallization process of calcium sulfate under microwave irradiation [11]. It has been reported that the explosion or burnout of reactants has been caused by hotspots when food, rubbers and ceramics are heated by microwave [12]. However, in some cases, we can make use of hotspots to accelerate chemical reactions. So a systematic simulation method needs to be developed in order to instruct the design of microwave chemistry reactors. Usually the hotspots occur on the place where temperature difference is large. Therefore it is necessary to analyze the information of temperature under microwave heating.

The formation of hotspots is due to three causes: (1) non-uniform distribution of materials with different dielectric losses; (2) non-uniform distribution of microwave field; (3) different thermoconductivities [13]. Conventionally, the researches on hotspots under microwave radiation focus on non-fluid objects such as solids. But, some of the chemical reactions are in the phase of liquid, but current simulations neglect the influence of fluid velocity. It is a reasonable approximation when the fluid flows very slowly or does not flow. However, given a large thermal gradient, the fluid convection or the buoyancy-driven-flow needs to be taken into account. Besides, stir is usually engaged in microwave chemical reactions, so it is necessary to take forced convection into calculating. In this paper, we simulate the process of the microwave heating on water with numerical method and research the conditions which have influence on temperature difference.

## 2. NUMERICAL SIMULATION OF MULTIPHYSICS AND FORMULATION

Now a coupling method needs to be developed so as to study the interaction process of electromagnetic field, fluid field and thermal field. In this paper, the coupled Maxwell's equations, fluid field equations and heat transport equations were solved by Finite-Element Method. The calculation model is shown in Fig. 1.

The microwave oven has the size of  $0.267(\text{m}) \times 0.270(\text{m}) \times 0.188(\text{m})$ . The water is in the beaker. The water column is divided into two parts. The outer part has the radius  $r_1 = 0.040(\text{m})$ , the length  $l_1 = 0.050(\text{m})$  and the inner part has the radius  $r_2 = 0.03(\text{m})$ ,

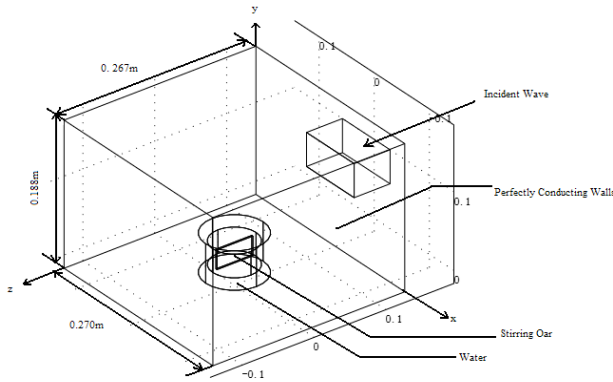


**Figure 1.** The numerical simulation model.

the length  $l_2 = 0.03$  (m). The origin of coordinate is located in the corner on the bottom surface of the cavity. The stirring oar has the size of  $0.050$  (m)  $\times$   $0.002$  (m)  $\times$   $0.025$  (m). The waveguide has the size of  $0.0864$  (m)  $\times$   $0.0432$  (m)  $\times$   $0.05$  (m). The microwave oven is a metallic box connected to a  $2000$  (W),  $2.45$  (GHz) microwave source via a rectangular waveguide operating in the  $TE_{10}$  mode.

### 2.1. The Dielectric Properties

The problem of microwave heating is directly related to electromagnetic fields, the temperature distribution within a dielectric material. Therefore, knowing the dielectric properties is essential for a theoretical prediction. An accurate evaluation of the electromagnetic fields, which determines microwave power dissipation within the dielectric material, is very important and crucial for the whole process. The microwave power dissipation represents the microwave power absorbed, which is eventually converted into thermal energy in dielectric materials. At the same time, the temperature will result in changes in dielectric properties. On the other hand, the dielectric properties will affect the microwave energy dissipation, thus effect variation of the temperature distribution. In this work the pure water is selected as the sample. The expression of dielectric property of the sample are defined as follow:

$$\epsilon_r = \epsilon' - j\epsilon'' \tag{1}$$

where  $\epsilon''$  accounts for dielectric losses. At a frequency of  $2.45$  GHz, The  $\epsilon_r$  changes with the temperature as follow [14], which is shown in Fig. 2:

## 2.2. Equations of Electromagnetic Field

In Fig. 1, the proposed model is based on the following assumptions:

- The rectangular port is excited by a transverse electric (TE) wave, which is a wave that has no electric field component in the direction of propagation. At an excitation frequency of 2.45 GHz, the TE<sub>10</sub> mode is the only propagating mode through the rectangular waveguide. The cutoff frequencies for the different modes are given analytically from the relation

$$(f_c)_{mn} = \frac{c}{2} \sqrt{\left(\frac{m}{a}\right)^2 + \left(\frac{n}{b}\right)^2} \quad (2)$$

where  $m$  and  $n$  are the mode numbers,  $a$  is the length of the waveguide port,  $b$  is the width of the waveguide port,  $f_c$  is cutoff frequency and  $c$  denotes the speed of light. For the TE<sub>10</sub> mode,  $m = 1$  and  $n = 0$ .

- The absorption of microwave energy by the cavity (including air) in the rectangular wave guide is negligible;
- The walls of a rectangular wave guide are perfect conductors;

The basic equations governing the electromagnetic field vectors are based on the well-known Maxwell curl relation. The differential form of Maxwell's equation can be expressed in terms of electric field intensity  $E$  and magnetic field intensity  $H$ . Maxwell's equations describing their space and time dependence are

$$\nabla \times \vec{E} = -\frac{\partial \vec{B}}{\partial t} \quad (3)$$

$$\nabla \times \vec{H} = \vec{J} + \frac{\partial \vec{D}}{\partial t} \quad (4)$$

$$\nabla \cdot \vec{D} = q \quad (5)$$

$$\nabla \cdot \vec{B} = 0 \quad (6)$$

where  $E$  and  $H$  are the electric field (V/m) and magnetic field (A/m),  $J$  is the current density current density (A/m<sup>2</sup>),  $D$  is the flux density (C/m<sup>2</sup>),  $q$  is the electric charge density (C/m<sup>3</sup>),  $t$  is the time(s) and  $B$  is the magnetic flux density (Wb/m<sup>2</sup>). The constitutive relations relating  $J$ ,  $D$  and  $B$  to  $E$  and  $H$  are

$$\vec{J} = \sigma \vec{E} \quad (7)$$

$$\vec{D} = \varepsilon \vec{E} \quad (8)$$

$$\vec{B} = \mu \vec{H} \quad (9)$$

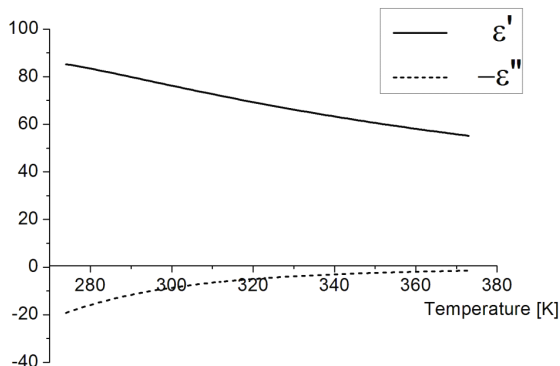


**Figure 2.**  $f = 2.45$  GHz, relative complex permittivity used in the calculations.

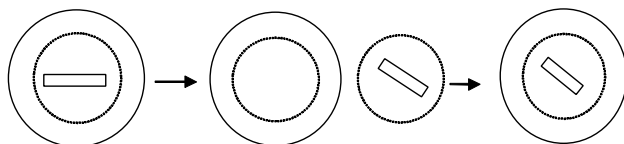


**Figure 3.** The modeling procedure of the stir in  $x$ - $z$  plane.

where the permittivity  $\epsilon$  (F/m), magnetic permeability  $\mu$  (H/m) and electric conductivity  $\sigma$  (S/m) are given by

$$\epsilon = \epsilon_0 \epsilon_r \tag{10}$$

$$\mu = \mu_0 \mu_r \tag{11}$$

$$\sigma = 2\pi f \tan \delta \tag{12}$$

where  $\tan \delta$  denotes dielectric loss coefficient (dimensionless),  $\epsilon_r$  is the relative permittivity (dimensionless),  $\mu_r$  is the relative magnetic permeability (dimensionless),  $\epsilon_0$  is the permittivity of free space (F/m),  $\mu_0$  is the magnetic permeability for free space (H/m).

Substituting Eqs. (6)–(10), Eqs. (2)–(5) become

$$\nabla \times \left( \mu_r^{-1} \nabla \times \vec{E} \right) - k_0^2 \left( \epsilon_r - \frac{j\sigma}{\omega \epsilon_0} \right) \vec{E} = 0 \tag{13}$$

$$k_0 = \omega \sqrt{\mu_0 \epsilon_0} \tag{14}$$

which are solved for the electric field vector  $E$  inside the waveguide and oven with the stipulated excitation at the rectangular port.  $j$  denotes

the imaginary unit,  $\omega$  is the angular frequency (rad/s). The model uses material parameters for air:  $\sigma = 0$  and  $\mu_r = \varepsilon_r = 1$ .

Boundary conditions in electromagnetic field:

- (a) Perfect electric conductor boundary condition: The walls of the oven and the waveguide are good conductors. The model approximates these walls as perfect conductors, represented by the boundary condition:

$$E_t = 0, \quad H_n = 0 \quad (15)$$

where subscripts  $t$  and  $n$  denote the components of tangential and normal directions, respectively.

- (b) Continuity boundary condition: Boundary conditions on the interface of the water are given as follows:

$$\vec{n} \times (\vec{H}_1 - \vec{H}_2) = 0 \quad (16)$$

$$\vec{n} \times (\vec{E}_1 - \vec{E}_2) = 0 \quad (17)$$

where  $\vec{n}$  denotes the unit vector of normal direction.

- (c) Port boundary condition: The rectangular port is excited by a transverse electric (TE) wave. The port power level and port phase of wave excitation at this port are 2000 W and 0, respectively. The power flux associated with a propagating electromagnetic wave is represented by the Poynting vector (W/m<sup>2</sup>):

$$S = \int (\vec{E} - \vec{E}_1) \cdot \vec{E}_1 / \int \vec{E}_1 \cdot \vec{E}_1 \quad (18)$$

The Poynting theorem allows the evaluation of the microwave power input. It is expressed as

$$P_{in} = \int_A S dA \quad (19)$$

where  $A$  denotes area (m<sup>2</sup>).

### 2.3. Fluid Flow Equations

The Navier-Stokes equation and mass conservation equation for fluid are given as

$$\rho \frac{\partial \vec{v}}{\partial t} + \rho (\vec{v} \cdot \nabla) \vec{v} = \nabla \left[ -p\vec{I} + \eta (\nabla \vec{v} + (\nabla \vec{v})^T) \right] + \vec{F} \quad (20)$$

$$\frac{\partial \rho}{\partial t} + \nabla \cdot (\vec{v} \rho) = 0 \quad (21)$$

In this paper, we considered the water as incompressible flow which  $\rho$  is a constant, therefore:

$$\nabla \cdot \vec{v} = 0 \tag{22}$$

where  $\rho$  denotes the density ( $\text{kg/m}^3$ ),  $\eta$  is the dynamic viscosity ( $\text{Pa}\cdot\text{s}$ ),  $v$  is the velocity ( $\text{m/s}$ ),  $p$  is the pressure ( $\text{Pa}$ ),  $F$  is the volume force ( $\text{N}$ ) and  $I$  is the unit tensor.

In order to achieve stir, we formulate the Navier-Stokes equations in a rotating coordinate system. Parts that are not rotated are expressed in the fixed coordinate system. The predefined coupling then takes care of the necessary administration to join the parts of the model that use a rotating coordinate system with the parts that are fixed. In Fig. 1, we divide the geometry of the fluid into two parts which are both rotationally invariant. As shown in Fig. 3, we specify the parts to model using a rotating frame and the ones to model using a fixed frame. Then do the coordinate transformation and the joining of the fixed and moving parts. The model equations are Navier-Stokes equations formulated in a rotating frame in the inner subdomain and in fixed coordinates in the outer one.

Boundary conditions in fluid field:

- (a) At the beaker's wall no-slip boundary conditions apply, the velocity is zero.  
Wall:  $\vec{v} = 0$
- (b) The boundary conditions for the stirring oar are no-slip clockwise rotation conditions which are given by  
Moving wall:  $\vec{v} = \vec{v}_w$ , where  $\vec{v}_w$  denotes the velocity of moving wall.
- (c) At the beaker outlet, we set the normal stress to zero.
- (d) The boundary condition on the interface between two parts of the fluid column is continuity which is given by the equation:

$$\vec{n} \left( \eta_1 \left( \nabla \vec{v}_1 + (\nabla \vec{v}_1)^T \right) - p_1 \vec{I} - \eta_2 \left( \nabla \vec{v}_2 + (\nabla \vec{v}_2)^T \right) + p_2 \vec{I} \right) = 0 \tag{23}$$

The value of the water's dynamic viscosity is small. Though the dynamic viscosity of water changes with the temperature, these changes nearly has no effect on temperature. Therefore we have the assumption that the effect of temperature on dynamic viscosity can be neglected and the dynamic viscosity is a constant.

## 2.4. Heat Transport Equations

The temperature of the fluid exposed to incident wave is obtained by solving the heat transport equation:

$$\rho C_p \frac{\partial T}{\partial t} + \nabla \cdot (-k \nabla T) = -\rho C_p \vec{v} \cdot \nabla T + Q \quad (24)$$

where  $\rho$  denotes the density ( $\text{kg}/\text{m}^3$ ),  $T$  is the temperature (K),  $v$  is the velocity (m/s),  $C_p$  is the heat capacity ( $\text{J}/(\text{kg} \cdot \text{K})$ ),  $k$  is the thermal conductivity ( $\text{W}/(\text{m} \cdot \text{K})$ ), and  $Q$  refers to the power density ( $\text{W}/\text{m}^3$ ) in the fluid that serves as a heat source.

Boundary conditions in thermal field:

- (a) The surroundings of the water are insulated

$$-\vec{n} \cdot (-k \nabla T) = 0 \quad (25)$$

- (b) At the upper surface, energy exchanges with the ambient air. In order to reduce complexity of the phenomena, we have the assumption that the effect of the container on temperature can be neglected.

The flow chart of the numerical simulation of multiphysics is shown in Fig. 4.

In this work, the pure water is selected as the sample. The parameters of water are shown in Table 1.

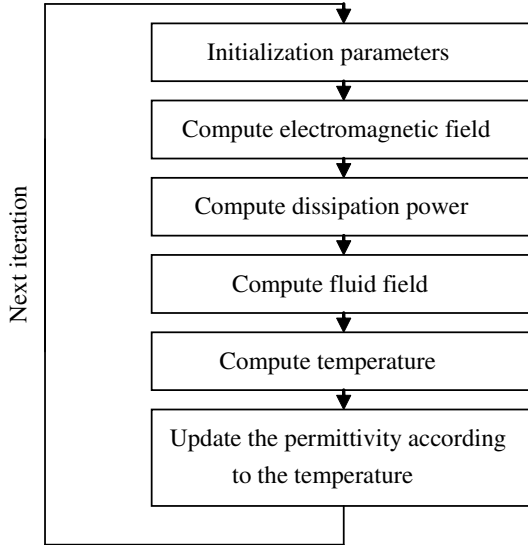


**Figure 4.** The flow chart of the numerical computation.



**Table 1.** The parameters of water used in the computations.

$\sigma = 0$	$k = 0.55 \text{ W}/(\text{m} \cdot \text{K})$
$\mu_r = 1$	$T_0 = 273 \text{ K}$
$\rho = 1000 \text{ kg}/\text{m}^3$	$C_p = 4200 \text{ J}/(\text{kg} \cdot \text{K})$
$\vec{F} = 0$	$\eta = 0.001 \text{ Pa} \cdot \text{s}$

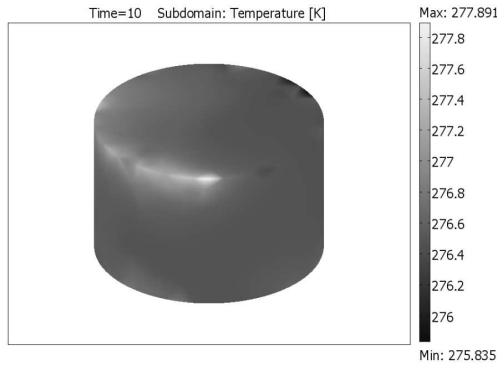


**Figure 5.** Power = 500 W, Temperature distribution in the water.

### 3. RESULTS AND DISCUSSION

People usually think that speeding up the stir can eliminate the temperature difference in the fluid during microwave heating. But in fact, temperature difference is related to many other factors such as power, dynamic viscosity, relative complex permittivity of the fluid which we will research in this paper.

#### 3.1. The Effect of Microwave Power

When the microwave power is 500 W, the temperature difference in the water which is stirred at a speed of 300 r/min for 10 seconds is shown in Fig. 5:

With temperature difference of 2.056 K, the temperature in the water is well-distributed under the microwave power of 500 W. Speeding up the stir can make temperature well-distributed under low microwave power.

In order to research the effect of high power on distribution of temperature difference, we heated the water under a high microwave power of 2000 W for 10 seconds at a speed of 20 r/min. Then we speed

up the stir. Fig. 6 is the temperature difference at different rotate speeds under high microwave power of 2000 W. The rotate speeds are 20 r/min, 60 r/min, 100 r/min, 300 r/min and 500 r/min, respectively.

Figure 6 shows that temperature difference decreases as we speed up the stir. When the rotate speed is slow, speeding up the stir has obvious effect on decreasing the temperature difference. But when the speed is fast enough, the effect of speeding up the stir on decreasing

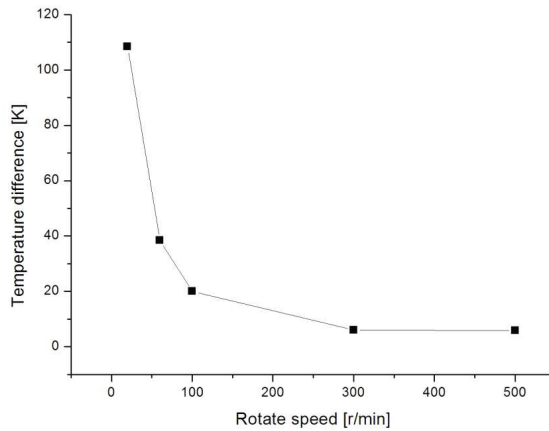


**Figure 6.** Time = 10 s, Power = 2000 W, Temperature difference at different rotate speeds under high microwave power.

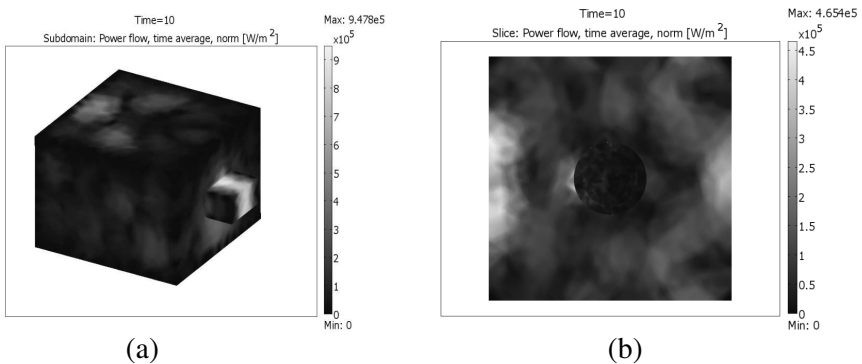


**Figure 7.** Power = 2000 W, The distribution of power flow norm: (a) Distribution of power flow in subdomain; (b) Distribution of power flow in  $x$ - $z$  plane ( $y = 0.025$ ).

temperature difference is weaker and weaker. At a speed of 300 r/min, the temperature difference is 6.038 K. Compared with 300r/min, the temperature difference at a speed of 500 r/min is 5.897 K which is nearly equal to 6.038 K. The temperature difference does not decrease any more.

Because 500 r/min is fast enough, we assume that 500 r/min is the limit of rotate speed. Fig. 7 and Fig. 8 show us the distribution of power flow norm and velocity field in  $x-z$  plane where  $y = 0.025$ . From Fig. 8, we can see that at the wall of the beaker, the velocity which plays a big part in thermal diffusion is nearly equal to zero. Fig. 9 is the simulation result of the temperature distribution in the water which is heated by microwave for 10 seconds at 500 r/min.

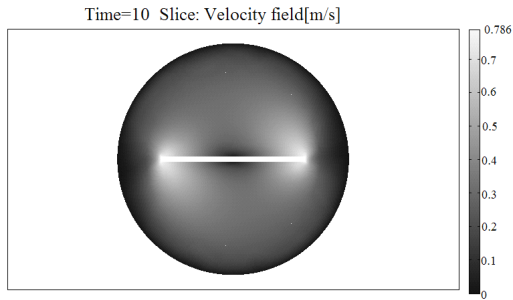


**Figure 8.** Power = 2000 W, The distribution of velocity in  $x-z$  plane ( $y = 0.025$ ).

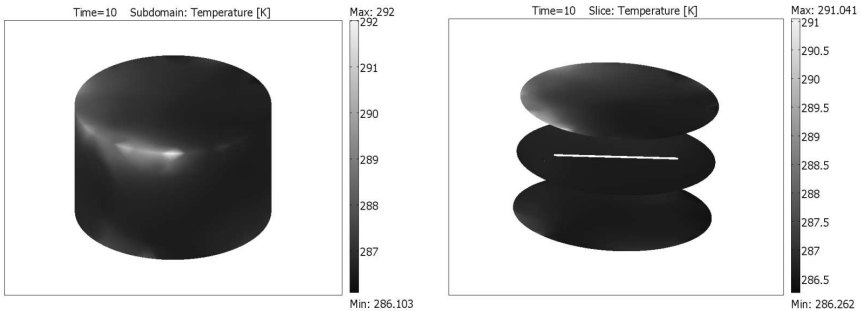


**Figure 9.** Power = 2000 W, Temperature distribution in the water at a rotate speed of 500 r/min.

In Fig. 9, we can see that inside the water, the temperature is well-distributed. And on the upper interface of the water the temperature is very high. Maybe under the condition of forced convection which is caused by stir, thermal diffusion is more favorable. But on the interface of the water and air, the velocity is nearly equal to zero. So the forced convection cannot take much effect.

### 3.2. The Effect of Relative Complex Permittivity

Because the problem of microwave heating is directly related to electromagnetic fields, the temperature distribution within a dielectric material. And the imaginary part of relative complex permittivity accounts for dielectric losses which determine microwave power dissipation within the dielectric material. The microwave power dissipation represents the microwave power absorbed, which is eventually converted into thermal energy in dielectric materials. Therefore, studying the effect of the imaginary part of relative complex permittivity on microwave heating is essential.

In Fig. 10, in order to study the effects of relative complex permittivity on distribution of temperature difference, we assume that the imaginary part of relative complex permittivity is a constant, so that we can compare the temperature difference when the water has different values of imaginary part of relative complex permittivity. We stir the water at a speed of 300 r/min and the imaginary part of permittivity are 10, 20, 30, 40, 50, respectively.

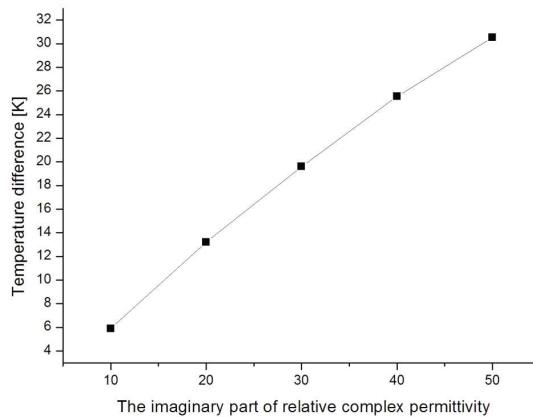


**Figure 10.** Time = 10 s, Power = 2000 W, Temperature difference with different imaginary parts of relative complex permittivity.

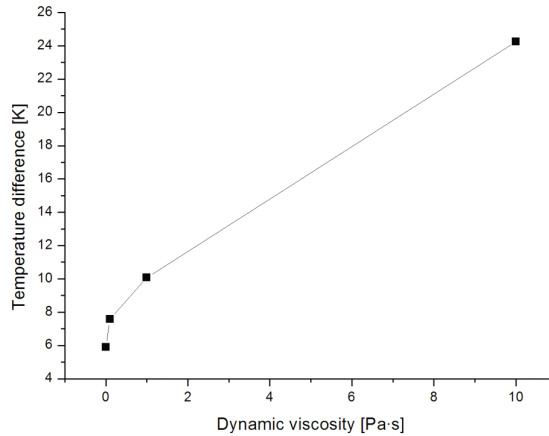


**Figure 11.** Time = 10 s, Power = 2000 W, Temperature difference with different dynamic viscosities.

In Fig. 10, we can see that with the value of the imaginary part of relative complex permittivity increases, the temperature in the water rises obviously. Even though the speed of stir is very fast, the temperature difference is also very large.

### 3.3. The Effect of Dynamic Viscosity

Considering the influence of dynamic viscosity on stirring, the water was heated by microwave at a rotate speed of 300 r/min with different dynamic viscosities such as 0.001 Pa · s, 0.1 Pa · s, 1 Pa · s and 10 Pa · s. Numerical simulation of the temperature difference in the water is shown in Fig. 11.

As seen in Fig. 11, with the same rotate speed, the smaller the value of dynamic viscosity is, the smaller the temperature difference is. When the value of dynamic viscosity is large, the temperature difference in the water is obvious even though the rotate speed is fast enough.

## 4. CONCLUSION

Electromagnetic field, fluid field and thermal field are successfully coupled to simulate the heating process of water under microwave by Finite-Element Method. Taking forced convection into account, this method has improved the simulation of multiphysics in fluid under

microwave heating. The results show that when the water is heated under high microwave power, speeding up the stir can improve the uniform of temperature. But if the rotate speed is fast enough, going on speeding up the stir cannot decrease the temperature difference any more. With large value of the imaginary part of relative complex permittivity, the temperature difference is obvious even though the rotate speed is fast enough. Maybe it is because that with high microwave power or large value of the imaginary part of relative complex permittivity, the speed of heating in the water is too fast. And on the interface of the water and air, the velocity of fluid flow is nearly equal to zero, so the thermal convection is weak and speeding up the stir cannot eliminate the situation that part of the water is heated too fast. Increasing the dynamic viscosity, the temperature difference in the water which is heated by microwave rises. When the value of dynamic viscosity is very large, the temperature difference is obvious even though the rotate speed is fast enough. Maybe the reason is that the heat transfer is weak because of slow speed of fluid convection with large value of dynamic viscosity. The coupled simulation of electromagnetic field, fluid field and thermal field provides a more accurate and effective method to simulate the heating process of chemical reactions under microwave, which makes it possible to further study the mechanisms of the special effects and non-thermal effects in microwave heating.

## ACKNOWLEDGMENT

This project was supported by National Science Foundation of China under Grant No. 60871064 and No. 61001019 and Research Fund for the Doctoral Program of Higher Education of China under Grant No. 20070610120.

## REFERENCES

1. Tavakoli, M. H., H. Karbaschi, and F. Samavat, "Computational modeling of induction heating process," *Progress In Electromagnetics Research Letters*, Vol. 11, 93–102, 2009.
2. Li, W., M. A. Ebadian, T. L. White, and R. G. Grubb, "Heat transfer within a concrete slab applying the microwave decontamination process," *ASME J. Heat Transfer*, Vol. 115, 42–50, 1993.
3. Clemens, J. and C. Saltiel, "Numerical modeling of materials processing in microwave furnaces," *Heat Mass Transfer*, Vol. 39, No. 8, 1665–1675, 1996.

4. Dibben, D. C. and A. C. Metaxas, "Frequency domain vs. time domain finite element methods for calculation of fields in multimode cavities," *IEEE Trans. Magn.*, Vol. 33, No. 2, 1468–1471, 1997.
5. Zhao, H. and I. W. Turner, "The use of a coupled computational model for studying the microwave heating of wood," *Appl. Math. Modeling*, Vol. 24, 183–197, 2000.
6. Bows, J. R., M. L. Patrick, R. Janes, A. C. Metaxas, et al., "Microwave phase control heating," *Food Sci. Technol.*, Vol. 34, 295–304, 1999.
7. Zhao, H., I. W. Turner, and G. Torgovnikov, "An experimental and numerical investigation of the microwave heating of wood," *Microwave Power Electromagn. Energy*, Vol. 33, 121–133, 1998.
8. Watanuki, J., "Fundamental study of microwave heating with rectangular wave guide," M.S. Thesis, Nagaoka University of Technology, Japan, 1998 (in Japanese).
9. Ratanadecho, P., K. Aoki, and M. Akahori, "A numerical and experimental investigation of the modelling of microwave melting of frozen packed beds using a rectangular wave guide," *Int. Comm. Heat Mass Transfer*, Vol. 28, 751–762, 2001.
10. Huang, K. M., Z. Lin, and X. Q. Yang, "Numerical simulation of microwave heating on chemical reaction in dilute solution," *Progress In Electromagnetics Research*, Vol. 49, 273–289, 2004.
11. Yang, X. Q. and K. M. Huang, "Study on the special effect of calcium sulfate crystallization under the irradiation of microwave," *Journal of Inorganic Materials*, Vol. 21, No. 2, 363–368, 2006.
12. Baker-Jarvis, J. and R. Inguva, "Dielectric heating of oilshales by monopoles and modified coaxial applicators," *Journal of Microwave Power and Electromagnetic Energy*, Vol. 23, No. 3, 160–170, 1984.
13. Mingos, D. M. P. and D. R. Baghurst, "Applications of microwave dielectric heating effects to synthetic problems in chemistry," *Chemical Society Reviews*, Vol. 20, No. 1, 1–47, 1991.
14. Torres, F. and B. Jecko, "Complete FDTD analysis of microwave heating processes in frequency-dependent and temperature-dependent media," *IEEE Microwave Theory and Techniques*, Vol. 45, No. 1, 108–117, 1997.